2012 IEEE International Conference on Robotics and Automation
RiverCentre, Saint Paul, Minnesota, USA
May 14-18, 2012

Planning and Control during Reach to Grasp using the Three Predominant UB Hand IV Postural Synergies

Fanny Ficuciello[1], Gianluca Palli[2], Claudio Melchiorri[2] and Bruno Siciliano[1]

***Abstract*— In this paper, a method to derive the three predominant synergies and their temporal weights for planning grasps of the UB Hand IV (University of Bologna Hand, version IV) is proposed. The method adopted to define the postural synergies from experiments is based on the kinematic structure of the robotic hand and on the taxonomy of the grasps of common objects. The control strategy, exploiting postural synergies, that drives the hand during reach to grasp is further described. During prehension the hand moves continuously in a configuration space of highly reduced dimensionality with respect to its degrees of freedom. The experiments confirm that the UB Hand IV works efficiently in a synergy based framework for grasp planning and prehension control. It is shown that the introduction of the third predominant synergy significantly improves the grasping synthesis and performance, especially for the adduction/abduction motion of the thumb.**

I. Introduction

Nowadays, the greatest effort of robotics research is going towards the design of a new generation of robots able to accomplish manipulation tasks in human-like ways so as to realize a proper and safe cooperation with humans. The undergoing research in the field aims at the reproduction of human abilities not only by means of anthropomorphic design but also by adopting human-inspired control strategies. Recent advances in neuroscience have shown that control of the human hand during grasping is dominated by movements in a continuous configuration space of highly reduced dimensionality with respect to the number of degrees of freedom. In [1] the principal component analysis (PCA) has been used to calculate the postural synergies from real-world data collected on a variety of human hand postures by means of a data glove. Moreover, the authors show that a wide set of hand postures during grasping operations evolve continuously within a linear space spanned by few postural synergies that account for most of the hand configurations variance, without distinguishing between power and precision grasps. In [2] it is shown that even if higher principal components account for a small percentage of the variance, they give critical details not only for the static grasp when the hand adapts to the object shape, but also for the act of preshaping during the grasp. In [3], [4], [5] the authors extend the concept of postural synergies to robotic hands showing how a similar dimensionality reduction can be used to derive comprehensive planning and controlling algorithms that produce stable grasps for a number of different robot hand models. Other applications have been made in order to simplify the design and analysis of robotic hand structures [6]. In [7] the authors investigate how the number and types of synergies are related to the possibility of controlling the contact forces and the object motion in grasping and manipulation tasks. In [8], using the definition of force-closure for underactuated hands and the definition of grasping force optimization, the authors investigate the role of different postural synergies in the ability of obtaining force closure grasps and the quality of the grasps in two case studies addressing a precision and a power grasp. In this paper, the eigengrasps for the UB Hand IV have been derived using the PCA by considering a set of 36 hand configurations among precision, intermediate and power grasps of common (for humans) objects contained in a comprehensive human grasp taxonomy [9]. All the data from experiments are obtained using a sensorless prototype of the UB Hand IV (Fig. 1) [10], an innovative robotic hand developed within the DEXMART project [11]. The reader is referred to [12] for a complete description of the finger kinematics and tendon network characteristics. The paper reports the method adopted to define from experiments the postural synergies for the UB Hand IV and the kinematics patterns performed adopting the three predominant synergies. Moreover, the temporal variation of the three synergies weights is exploited for real-time execution of the grasps. Experimental results show that the grasp planning and control of the UB Hand IV performed by using the three predominant postural synergies allows synthesizing and performing a wide set of grasps, throughout the whole grasp taxonomy, namely precision, intermediate and power grasps of objects with different

Fig. 1. The UB Hand IV prototype.

[1]Dipartimento di Informatica e Sistemistica, Università di Napoli Federico II, 80125 Napoli, Italy, email: {*fanny.ficuciello, bruno.siciliano*}*@unina.it*.

[2]Dipartimento di Elettronica, Informatica e Sistemistica, Alma Mater Studiorum Università di Bologna, 40136 Bologna, Italy, email: {*gianluca.palli, claudio.melchiorri*}*@unibo.it*.

This research has been partially funded by the EC Seventh Framework Programme (FP7) under grant agreement no. 216239 for the IP DEXMART (DEXterous and autonomous dual-arm/hand robotic manipulation with sMART sensory-motor skills: A bridge from natural to artificial cognition).

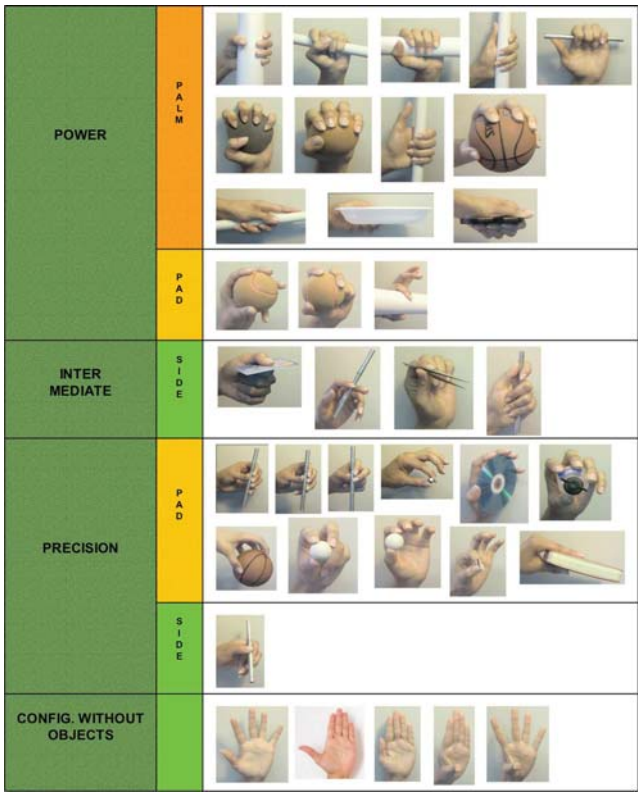

Fig. 2. Reference set of comprehensive human grasps and open hand configurations used for the PCA.

shapes and dimensions. With respect to a previous work [13], in this paper the experiments for deriving the postural synergies subspace have been repeated using the postures set represented in Fig. 2. Additional experiments have been carried out and the analysis of the data shows that the introduction of the third predominant synergy significantly improves the grasp synthesis and performance, especially with regard to the improvement of the adduction/abduction motion of the thumb. The paper is organized as follows: Section II provides the description of the method adopted for deriving the hand postural synergies and the description of the kinematic patterns of the three predominant ones. Moreover, the method to obtain the temporal weights of these synergies for grasps planning and the method to control the hand exploiting postural synergies is further described. In Section III the experimental results about the use of the three predominant synergies for the synthesis of grasps are reported, together with a comparison with the use of the two synergies only. Finally, Section IV provides conclusions and sketches future work.

II. Postural Synergies of the UB Hand IV

The postural synergies describe patterns occurring at the joint displacement level. In [1], the authors measure a set of static human hand postures by recording 15 joint angles and, by means of the PCA, they show that the first two principal components account for $>80\%$ of the hand postures. Thus the use of the principal components, also called postural synergies, holds great potential for robot hand control, implying a substantial reduction of the grasp synthesis problem dimension with respect to the case of considering the entire number of robotic hand Degrees of Freedom (DoFs). In this work the third synergy is experimentally obtained and evaluated, with further considerations about the adduction/abduction motion of the thumb. Indeed, by exploiting the third synergy, the movement of adduction/abduction of the thumb covers the whole range of joint limits without violating the limits of the other joints. This improves the correct opposition of the thumb and allows synthesizing and executing more precisely complex grasps and reproducing the set of postures adopted to derive the eigengrasps with higher accuracy with respect to the case in which only two synergies are used.

The first two synergies found for the UB Hand VI account for $>77\%$ of the hand postures, thus matching quite well the results reported in [1]. Therefore, since the three predominant postural synergies account for $>85\%$ of the hand postures, a robot hand control strategy that uses also the third synergy will significantly improve the grasping performance, as the experiments reported in this paper show.

A. PCA Analysis

The postural synergies of the UB Hand IV have been derived using the PCA on the basis of a properly chosen reference set of grasps. Since the UB Hand IV kinematics is quite close to the human's one, the choice of the reference set of postures has been made by taking into account the most common human grasps considered in the grasp taxonomy literature [14]. In detail the grasping action evaluated in [9] has been used as a guide. A set of grasps of cylindrical and circular objects involving different number of fingers has been considered. Following the taxonomy in [15], a comprehensive hierarchical human grasp classification used for the PCA is reported in Fig. 2. The three main clusters, i.e. power, intermediate side and precision grasps have been further split into three groups (palm, pad, and side) depending on which part of the hand is in contact with the object. Furthermore, a suitable number of open hand configurations with different positions of the thumb and of the adduction/abduction fingers joint has been added in order to find synergies that allow the hand to moves continuously also toward open hand configurations which are equally important to reach and grasp the objects. A total amount of $n = 36$ hand configurations has been evaluated to derive the fundamental eigenpostures. Each grasp configuration of the postures reference set has been experimentally reproduced with UB Hand IV as close as possible to a natural human-like grasp. The vector $\mathbf{c}_i$ of the joint angle values corresponding to each reproduced grasp has been measured and collected in the configurations matrix $\mathbf{C} = \{\mathbf{c}_i \mid i = 1 \ldots n\}$. Once the vector $\bar{\mathbf{c}}$ representing the mean hand position in the grasp configurations space (zero-offset position) has been computed, the PCA has been performed on the covariance centered matrix as referred in [13]. The principal component which arise from the PCA are the postural synergy, i.e. the directions of variance of the

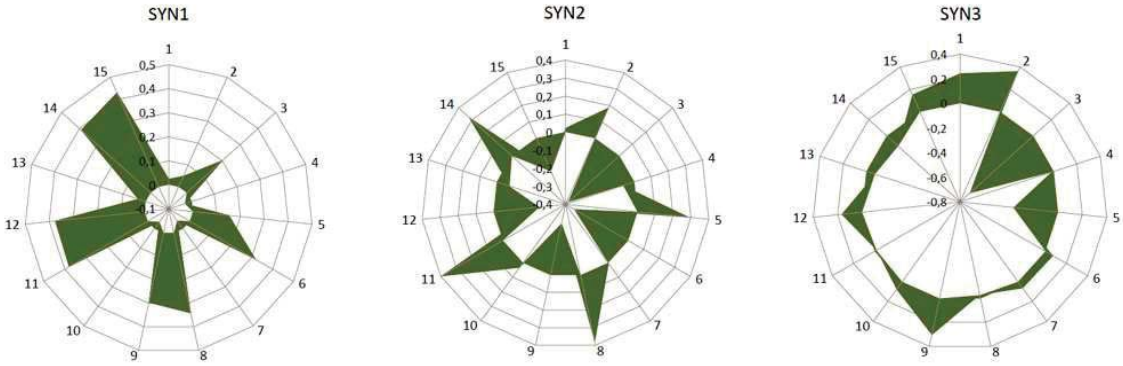

Fig. 3. In this figure, the angular change in degrees for each joint due to a positive unitary variation in α_1, α_2, and α_3 for the first three synergies is represented. The adduction/abduction, proximal and medial flexion joints are indicated from 1 to 3 for the thumb, from 4 to 6 for the index finger, from 7 to 9 for the middle finger, from 10 to 12 for the ring finger and finally from 13 to 15 for the little finger.

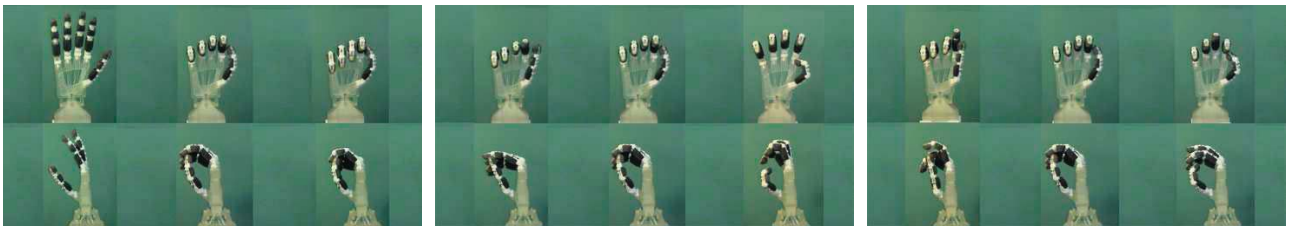

(a) First postural synergy. (b) Second postural synergy. (c) Third postural synergy.

Fig. 4. Representation of the UB Hand IV postural synergies. On the top of each figure, from left to right, a sequence of hand postures going form the minimum to the maximum configuration are represented. On the bottom the lateral views are reported.

data represented in the $(h \times h)$ orthogonal matrix $\mathbf{E}$ whose columns are in order of decreasing component variance. Since the three principal components account for >85% of the postures, the posture matrix $\mathbf{C}$ can be reconstructed with high accuracy by adopting the matrix

$$\hat{\mathbf{E}} = [\mathbf{e}_1 \ \mathbf{e}_2 \ \mathbf{e}_3] \tag{1}$$

composed by the three principal components $\mathbf{e}_1$, $\mathbf{e}_2$ and $\mathbf{e}_3$ of $\mathbf{E}$ as a base of the robotic hand configuration space, thus allowing the control of the robotic hand motion in a configuration space of highly reduced dimensions with respect to the degrees of freedom of the hand itself. Each hand's grasp postures $\mathbf{c}_i$ can be obtained by a suitable selection of the weights $[\alpha_{1,i} \ \alpha_{2,i} \ \alpha_{3,i}]^T$ of the postural synergies. Therefore, the projection $\hat{\mathbf{c}}_i$ of each robotic hand configuration $\mathbf{c}_i$ on the postural synergies subspace can be evaluated as

$$\hat{\mathbf{c}}_i = \bar{\mathbf{c}} + \hat{\mathbf{E}} \begin{bmatrix} \alpha_{1,i} \\ \alpha_{2,i} \\ \alpha_{3,i} \end{bmatrix}. \tag{2}$$

When the weights of the synergies are zero, the hand posture corresponds to the zero-offset position $\bar{\mathbf{c}}$. The vectors of the three synergies and the zero-offset vector of the UB Hand IV are reported in Tab. I. The circular graphs represented in Fig. 3 are a useful tool for identifying the joints whose rotations are more involved in each synergy. From left to right, the angular variations in degrees for each joint due to a unitary variation of the corresponding synergy weight is represented for the first, the second and the third synergy. It is easy to observe how the adduction/abduction thumb joint motion (joint #1) is more involved in the third synergy rather than in the first two. Moreover, in the third synergy the movement of the index and of the thumb are more engaged than for the other fingers. This justifies the use of the third synergy in order to grasp objects more precisely, especially for precision grasps and intermediate side grasps, where the position of the thumb and of the index is crucial, as the experiments reported in Sect. III demonstrate. The three synergies, shown in Fig. 4(a), 4(b) and 4(c), are now analyzed in detail, referring to the minimum and maximum configuration of each synergy as the hand configurations obtained by means of, respectively, the minimum and maximum value of the corresponding synergy weights without violating the joint limits ([13]).

B. First Synergy

With reference to the first postural synergy (column $\mathbf{e}_1$ in Tab. I), in the minimum configuration the proximal and medial flexion joint angles of all the fingers are all almost zero and increase their value during the motion toward the maximum configuration. The adduction/abduction movements are not very involved in this synergy. In Fig. 4(a) the minimum, zero-offset and maximum configuration in frontal and lateral view of the first postural synergy are represented.

Fig. 5. Reproduced power grasps from the reference set of postures using the first three synergies.

C. Second Synergy

The second postural synergy (column $\mathbf{e}_2$ in Tab. I) is characterized by a movement in opposite directions of the proximal and medial flexion joints. In this synergy, the adduction/abduction movements of all the fingers are more involved with respect to the first synergy for the index and the little finger. In Fig. 4(b) the minimum, zero-offset and maximum configurations of the second postural synergy are depicted in frontal and lateral views.

D. Third Synergy

In the third postural synergy (column $\mathbf{e}_3$ in Tab. I) the movement involves especially the index and the thumb. Thanks to this synergy, the movement of adduction/abduction of the thumb covers the whole joint range without violating other joint limits. This characteristic is crucial because the correct index/thumb opposition allows increasing the grasp accuracy, and thus achieving more stable grasps. This justifies the use of three predominant synergies for the hand control in order to improve the grasp performance. Finally, the excursion of the angles of adduction/abduction of the middle and ring fingers are quite involved in this synergy, more than in the first two. In Fig. 4(c) the minimum, zero-offset and maximum configuration in frontal and lateral views of the third postural synergy are represented.

E. Control with postural synergies

In order to perform the desired grasp, the value of the three eigenpostures weights $[\alpha_1 \ \alpha_2 \ \alpha_3]^T$ are computed by projection of the desired grasp posture in the synergies subspace:

$$\begin{bmatrix} \alpha_{1,i} \\ \alpha_{2,i} \\ \alpha_{3,i} \end{bmatrix} = \hat{\mathbf{E}}^{\dagger} \left(\mathbf{c}_i - \bar{\mathbf{c}} \right) \tag{3}$$

where $\hat{\mathbf{E}}^{\dagger}$ means the pseudo-inverse of the base matrix $\hat{\mathbf{E}}$. It is straightforward to note that the motions shown in Fig. 4(a), 4(b) and 4(c), derived by considering separately the three synergies, are obtained from (2) by assuming $\alpha_2 = 0$ and $\alpha_3 = 0$ for the first synergy, $\alpha_1 = 0$ and $\alpha_3 = 0$ for the second synergy, and finally $\alpha_1 = 0$ and $\alpha_2 = 0$ for the third synergy.

TABLE I

FIRST THREE EIGENPOSTURES AND ZERO OFFSET VECTORS OF THE UB HAND IV POSTURAL SYNERGIES SUBSPACE (DATA IN DEGREES).

		$\mathbf{e}_1$	$\mathbf{e}_2$	$\mathbf{e}_3$	$\bar{\mathbf{c}}[deg]$
Thumb	adduction/abduction	0.0282	0.0235	-0.2454	-0.833
	proximal	0.0674	0.1874	-0.3639	20.5
	medial	0.2004	-0.3853	0.6991	34.7
Index	adduction/abduction	-0.0266	-0.0647	0.0228	2.92
	proximal	0.1575	0.2893	0.3648	34.9
	medial	0.3220	-0.3494	-0.0735	50.5
Middle	adduction/abduction	-0.0404	0.0069	-0.0675	-0.694
	proximal	0.3405	0.3794	0.0304	41.4
	medial	0.2999	-0.2948	-0.3034	42.2
Ring	adduction/abduction	-0.0374	0.0343	-0.0778	-1.11
	proximal	0.3775	0.3977	0.0200	45.5
	medial	0.3766	-0.2568	-0.1675	49.2
Little	adduction/abduction	0.0364	-0.0738	0.0720	0.694
	proximal	0.3892	0.3213	0.1273	48.7
	medial	0.4235	-0.2026	-0.1491	51.7

Fig. 6. Reproduced precision grasps from the reference set of postures using the first three synergies.

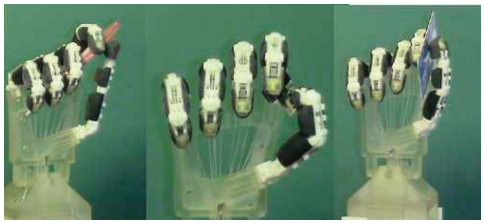

Fig. 7. Reproduced intermediate side grasps from the reference set of postures using the first three synergies.

III. EXPERIMENTAL EVALUATION OF THE SYNERGY-BASED GRASP SYNTHESIS

The video footage to this paper shows the pattern's motion of each synergy and the results of the grasp experiments. The temporal value of the weights α_1, α_2, α_3 during grasp operations has to be chosen in such a way that, starting from the zero-offset position $\bar{\mathbf{c}}$ (i.e. $\alpha_1 = \alpha_2 = \alpha_3 = 0$), the hand opens during the reach in preparation for object grasp, and then closes reaching a suitable shape determined from (3) and depending on the original grasp configuration $\mathbf{c}_i$ for the considered object. In the open-hand configuration, namely $\mathbf{c}_0$, all the flexion joint angles are close to zero, and the corresponding values of α_1, α_2 and α_3 can be determined from (3) by posing $\mathbf{c}_i = \mathbf{c}_0$.

The intermediate values of the synergy weights have been determined by assuming a suitable time interval for the grasp operation (six seconds for the whole reach to grasp phase,

TABLE II

SYNERGY WEIGHTS OF THE GRASPS FROM THE REFERENCE SET OF POSTURES.

Conf.	C1	C2⋆	C3	C4⋆	C5	C6	C7	C8
α_1	0.90	63.7	64.7	38.0	21.9	42.7	53.1	68.2
α_2	-3.47	28.1	-24.5	36.5	-33.6	-5.76	-8.21	-8.66
α_3	7.06	3.61	7.95	-21.2	-65.9	-2.33	-4.68	-8.56
Conf.	C9◇	C10⋆	C11⋆	C12⋆	C13◇	C14⋆	C15	C16⋆
α_1	-30.8	-4.00	58.8	12.3	-7.89	-18.9	8.86	63.7
α_2	-12.0	-117	9.39	-63.5	-59.0	8.47	1.36	39.3
α_3	21.4	-2.30	44.3	-14.0	27.6	0.15	-23.7	-8.38
Conf.	C17	C18	C19⋆	C20⋆	C21	C22	C23◇	C24
α_1	13.7	42.7	67.4	-29.8	-18.4	-30.4	82.8	39.8
α_2	44.2	-43.2	28.4	122	-0.103	-30.2	2.58	23.3
α_3	-37.6	-13.2	16.0	25.3	17.7	11.2	31.7	18.3
Conf.	C25◇	C26	C27◇	C28	C29	C30	C31⋆	C32
α_1	35.4	65.3	75.9	81.8	-103	-120	26.3	-134
α_2	-17.8	1.82	19.8	26.4	-28.0	29.5	-0.933	4.10
α_3	27.6	18.8	-68.0	-20.3	27.8	18.7	31.0	-9.15
Conf.	C33	C34	C35	C36				
α_1	-134	-127	-134	-135				
α_2	4.20	18.3	4.96	3.73				
α_3	-10.2	-36.5	-5.04	-5.26				

TABLE III

ADDUCTION/ABDUCTION THUMB JOINT ANGLE ERROR (IN DEGREES) IN THE REPRODUCED GRASPS FROM THE REFERENCE SET OF POSTURES OBTAINED USING TWO AND THREE SYNERGIES.

Conf.	C1	C2⋆	C3	C4⋆	C5	C6	C7	C8
two syn	9.11	11.6	9.59	8.89	11.0	9.76	9.53	9.11
three syn	7.38	10.7	11.5	3.69	5.16	9.19	8.38	7.01
Conf.	C9◇	C10⋆	C11⋆	C12⋆	C13◇	C14⋆	C15	C16⋆
two syn	8.02	6.30	11.0	12.0	7.56	8.83	10.5	1.88
three syn	2.77	6.87	0.17	8.54	0.77	8.80	4.73	3.94
Conf.	C17	C18	C19⋆	C20⋆	C21	C22	C23◇	C24
two syn	9.41	9.35	8.26	11.2	8.65	7.60	11.6	10.8
three syn	0.186	12.6	12.2	4.97	4.30	4.84	3.79	6.33
Conf.	C25◇	C26	C27◇	C28	C29	C30	C31⋆	C32
two syn	9.74	8.95	8.23	7.91	5.59	6.48	9.89	14.5
three syn	2.98	13.6	8.46	2.93	1.22	1.88	2.28	12.3
Conf.	C33	C34	C35	C36				
two syn	14.5	14.0	5.50	5.45				
three syn	12.0	5.02	6.74	6.74				

three seconds for both the opening and closing phases) and by linear interpolation of the α_1, α_2 and α_3 values in the three reference configurations $\{\bar{\mathbf{c}},\ \hat{\mathbf{c}}_0,\ \hat{\mathbf{c}}_i\}$, where $\hat{\mathbf{c}}_i$ is the i-th object grasp configuration obtained by projection on the synergies subspace by means of (3).

The linear combination of the three synergies allows a power grasp of both cylinders and spheres of different dimensions by means of suitable opposition of the thumb, see Fig. 5. In Fig. 6, the performance of precise grasp operations is reported considering different objects and involving different number of fingers.

The reproduced intermediate side grasps from the reference set of postures is depicted in Fig. 7. By observing the first image from the left (pen, Configuration C27 in Tab. II) of Fig. 7, it is interesting to note that this posture is very close to the minimum configuration of the third synergy; indeed the weight of the third synergy is high with respect

TABLE IV

AVERAGE JOINT ANGLE ERRORS (IN DEGREES) IN THE REPRODUCED GRASPS FROM THE REFERENCE SET OF POSTURES OBTAINED USING TWO AND THREE SYNERGIES.

Conf.	C1	C2⋆	C3	C4⋆	C5	C6	C7	C8
two syn	1.81	1.84	1.83	2.70	4.89	2.25	2.24	2.12
three syn	1.75	1.82	1.75	2.30	2.16	2.24	2.22	2.05
Conf.	C9◇	C10⋆	C11⋆	C12⋆	C13◇	C14⋆	C15	C16⋆
two syn	2.21	1.38	3.48	1.90	2.64	1.63	3.62	1.56
three syn	1.69	1.37	1.84	1.65	1.89	1.63	3.26	1.46
Conf.	C17	C18	C19⋆	C20⋆	C21	C22	C23◇	C24
two syn	4.11	2.01	3.20	2.19	2.06	3.78	2.77	2.34
three syn	3.26	1.81	3.02	1.40	1.68	3.70	1.79	1.99
Conf.	C25◇	C26	C27◇	C28	C29	C30	C31⋆	C32
two syn	2.95	2.31	4.83	4.27	3.29	4.05	2.60	2.00
three syn	2.31	1.94	1.66	4.05	2.72	3.86	1.57	1.90
Conf.	C33	C34	C35	C36				
two syn	1.92	4.99	1.99	1.70				
three syn	1.80	4.35	1.97	1.66				

to the other grasps, and thus the use of the third synergy is essential for this performance. Experimental results reveal that the use of the third synergy allows reproducing several grasp configurations more precisely than in the case of using two synergies only [13], and in particular it allows a better control of the adduction/abduction motion of the thumb. In fact, by looking at Tab. III where the joint errors in the cases of using two and three synergies for the control of the hand are compared, it is possible to note that the use of the three predominant synergies reduces the error on the angular position of the adduction/abduction thumb joint for almost all the 36 configurations with respect to the case in which only two synergies are used. In Tab. III, the grasp configurations executed by using only two synergies are marked with a star, while the new grasp configurations that have been performed successfully adding the third synergy are marked with a diamond. This table shows that, by introducing the third predominant synergy, the joint angle error of the thumb is reduced for almost all the grasps configurations marked with a star, except for C10 (box) C16 (credit card) and C19 (pen). Nevertheless, a global improvement obtained using also the third synergy is evident while observing the average joint angle errors reported in Tab. IV. Only for Configuration C14 no improvement has been obtained and this is confirmed by the very small value of the third synergy weight (Tab. II); this means that the third synergy gives almost no contribution to the variance of this posture. The improvement on the adduction/abduction thumb joint angle using the third synergy is very clear at least for the configurations marked with a diamond. For what concerns Configuration C27 (pen, intermediate side grasp), the improvement can be seen mainly in the error average and is spread on the thumb and index joints. These results show that the use of the third synergy allows grasping objects more precisely, especially when the position of the thumb and index is crucial, as in the case of precision grasps. The confirmation of this is given by the observation that the configurations marked with a diamond correspond to

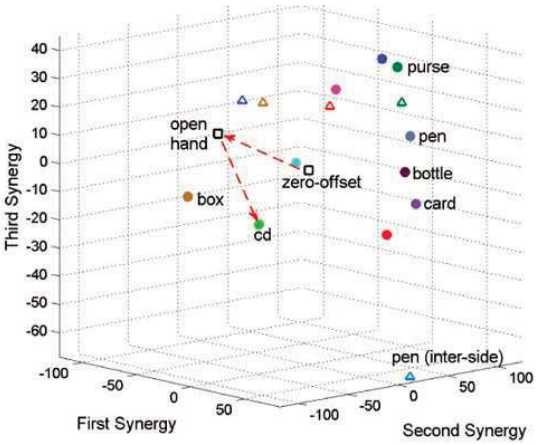

Fig. 8. The distribution of hand postures in the space of the first three postural synergies is represented, distinguishing between the object graspable also using the first two synergies only (full bullets) and the objects graspable thanks to the use of the third synergy (triangles).

precision grasps, except for C27. In Fig. 8, the distribution of the synergy weights adopted for executing the grasping experiments is shown in the space of the three predominant eigengrasps, and an example of a complete hand trajectory computed by linear interpolation of the synergies weights in the three reference configurations for the grasp of a generic object (a CD) is reported by the dashed line. For the sake of clarity, in Fig. 8 only the weights of the grasps obtained during the experiments are reported, and only some of them are named. In this figure the full bullets represent the final configuration weights corresponding to the grasps performed also in the previous work [13]. The triangles represent the final configuration weights corresponding to the objects that have been grasped thanks to the use of the third synergy also. In Fig. 9 two grasp configurations executed using both two and three synergies are represented. From left to right the first pictures of the ball and of the CD are the ones executed using three synergies. From these pictures, the improvement on the position of the thumb, thanks to the introduction of the third synergy in the hand control, can be noticed.

IV. Conclusion and Future Work

In this paper the experimental evaluation of the three predominant UB Hand IV postural synergies has been presented. Using the PCA, the UB Hand IV eigenpostures have been found taking into account a suitable set of hand postures. The kinematic patterns of the first three postural synergies are described and the use of the third synergy is added to improve a previous work [13]. Since, in this set of experiments the three predominant postural synergies account for $>85\%$ of the hand postures with respect to the $>77\%$ covered by the first two synergies only, it has been shown that the control strategy that uses also the third synergy improves the grasping tasks carried out with only two synergies and allows synthesizing complex grasps more accurately. Future work will focus on using also additional eigenpostures for fine manipulation through the integration of the contact force measurements.

Fig. 9. Comparison between two grasps configuration executed using both two and three synergies. From left to right the first pictures of the ball and of the cd are the ones executed using three synergies.

Acknowledgments

The authors want to thank all those who have contributed in the recent years to the development of the UB Hand IV prototype. Further, the support of Umberto Scarcia and Ugo Fabrizi during the experiments described in this paper is gratefully acknowledged.

References

[1] M. Santello, M. Flanders, and J. Soechting, "Postural hand synergies for tool use," *Journal of Neuroscience*, vol. 18, no. 23, pp. 10 105–10 115, 1998.

[2] C. Mason, J. Gomez, and T. Ebner, "Hand synergies during reach-to-grasp," *Journal of Neurophysiology*, vol. 86, no. 6, pp. 2896–2910, 2001.

[3] M. Ciocarlie, C. Goldfeder, and P. Allen, "Dimensionality reduction for hand-independent dexterous robotic grasping," in *Proc. IEEE/RSJ International Conference on Intelligent Robots and Systems*, San Diego, 2007, pp. 3270–3275.

[4] M. Ciocarlie and P. Allen, "Hand posture subspaces for dexterous robotic grasping," *International Journal of Robotics Research*, vol. 28, no. 7, pp. 851–867, 2009.

[5] ——, "On-line interactive dexterous grasping," in *Proc. 6th International Conference on Haptics: Perception, Devices and Scenarios*, Madrid, 2008, pp. 104–113.

[6] C. Brown and H. Asada, "Inter-finger coordination and postural synergies in robot hands via mechanical implementation of principal components analysis," in *Proc. IEEE/RSJ Interational Conference on Intelligent Robots and Systems*, San Diego, 2007, pp. 2877–2882.

[7] D. Prattichizzo, M. Malvezzi, and A. Bicchi, "On motion and force controllability of grasping hands with postural synergies," in *Proc. of Robotics: Science and Systems*, Zaragoza, 2010.

[8] M. Gabiccini and A. Bicchi, "On the role of hand synergies in the optimal choice of grasping forces," in *Proc. of Robotics: Science and Systems*, Zaragoza, 2010.

[9] J. Romero, T. Feix, H. Kjellstrom, and D. Kragic, "Spatio-temporal modelling of grasping actions," in *Proc. IEEE/RSJ International Conference on Intelligent Robots and Systems*, Taipei, 2010, pp. 2103–2108.

[10] G. Berselli, G. Borghesan, M. Brandi, C. Melchiorri, C. Natale, G. Palli, S. Pirozzi, and G. Vassura, "Integrated mechatronic design for a new generation of robotic hands," in *Proc. IFAC Symposium on Robot Control*, Gifu, Japan, 2009.

[11] DEXMART Project website, http://www.dexmart.eu/.

[12] G. Borghesan, G. Palli, and C. Melchiorri, "Design of tendon-driven robotic fingers: Modelling and control issues," in *Proc. IEEE International Conference on Robotics and Automation*, Anchorage, 2010, pp. 793–798.

[13] F. Ficuciello, G. Palli, C. Melchiorri, and B. Siciliano, "Experimental evaluation of postural synergies during reach to grasp with the UB Hand IV," in *Proc. IEEE/RSJ International Conference on Intelligent Robots and Systems*, San Francisco, 2011, pp. 1775–1780.

[14] M. Cutkosky, "On grasp choice, grasp models, and the design of hands for manufacturing tasks," *IEEE Transactions on Robotics and Automation*, vol. 5, no. 3, pp. 269–279, 1989.

[15] T. Feix, R. Pawlik, H. Schmiedmayer, J. Romero, and D. Kragic, "The generation of a comprehensive grasp taxonomy," in *Robotics, Science and Systems, Workshop on "Understanding the Human Hand for Advancing Robotic Manipulation"*, Washington, 2009.